Low voltage operating organic light emitting transistors with efficient charge blocking layer

Alexandre Bachelet, Marion Chabot, Abduleziz Ablat, Kazuo Takimiya, Lionel Hirsch, Mamatimin Abbas

Low Voltage Operating Organic Light Emitting Transistors with efficient charge blocking layer

Alexandre Bachelet,[1] Marion Chabot,[1] Abduleziz Ablat,[1] Kazuo Takimiya,[2,3] Lionel Hirsch,[1] Mamatimin Abbas[1,*]

[1]Univ. Bordeaux, IMS, CNRS, UMR 5218, Bordeaux INP, ENSCBP, F-33405 Talence, France
[2]Emergent Molecular Function Research Team, RIKEN Center for Emergent Matter Science (CEMS), 2-1 Hirosawa, Wako, Japan
[3]Department of Chemistry, Graduate School of Science, Tohoku University, 6-3 Aoba, Aramaki, Aoba-Ku, Sendai, Japan
**Corresponding author: mamatimin.abbas@ims-bordeaux.fr*

Abstract: Charge injection/blocking layers play important roles in the performances of organic electronic devices. Their incorporation into organic light emitting transistors has been limitted, due to generally high operating voltages (above 60 V) of these devices. In this work, two hole blocking molecules are integrated into tris-(8-hydroxyquinoline) aluminum (Alq_3) based light emitting transistors under operating voltage as low as 5 V. The effects of hole blocking and electron injection are decoupled through the differences in the energy levels. Significantly improved optical performance is achieved with the molecule of suitable energy level for electron injection. Surprisingly, a decreased performance is observed in the case of another hole blocking molecule evidencing that charge injection overweighs charge blocking in this device architecture.

Key words: organic light emitting transistor; low voltage operation; hole blocking layer

Electronic devices based on organic semiconductors (OSC) have been well studied over the last decades as they enable specific applications those of which their inorganic counterparts cannot fulfil. [1,2] These devices can be easily processed with potential low cost. They can be large area, light weight and flexible. [3–5] An interesting and aspiring device in this field is organic light emitting transistor (OLET), a multifunctional optoelectronic device. It combines the electrical switching function of a field effect transistor (FET) with the light emission property of a light emitting diode (LED). [6,7] The potential applications of such a device are numerous, from active matrix display to even electrically pumped lasing. [8,9] Since the first report on OLET, there has been enormous progress in this field. [10–14] To further enhance the performance of these devices, incorporation of interfacial layers such as charge injection and blocking layers is essential, as they play rather important role in device performances of organic electronic devices being almost indispensable in some cases, such as in organic LEDs. [24] However, one limitation thus far has been the rather high operating voltages of OLETs in many reported studies (even above 100 V in some cases). [15–17] Such an operating condition limits the potential areas of their application (displays require below 10 V operations) and restrains the efficiency and stability of these devices under strong electrical stress, but also obscures the role of charge injection/blocking layers. That is why developing low voltage operating OLETs can be regarded as a major focus in research towards technological applications. Two aspects have to be considered to realize low voltage operating OLETs. One is to apply high mobility transport layers, such as metal oxides, small molecules or polymers. [18–20] Another is that the capacitance of the dielectric layer should be augmented, either by minimizing the thickness or using high-k dielectrics. [21,22] Up to now, only one work reported OLET operating below 10 V. [23] Low voltage operating devices provide ideal platform to explore the potential of charge injection/blocking layers in further enhancing the electrical and optical performances of OLETs. However, incorporation of them are lacking among those very few OLET devices operating at relatively low voltages. [23,25]

In this work, we first realized low voltage operating OLETs using high hole mobility 2,9-didecylnaphtho[2,3-b:2',3'-f]thieno[3,2-b]thiophene (C_{10}-DNTT) as transport layer and anodized Al_2O_3 as dielectric layer. [26,27] Operating voltage was reduced to as low as 5 V, which allowed us to unambiguously investigate the effect of hole blocking layers in our OLETs. Two molecules: 2,2',2''-(1,3,5-benzinetriyl)-tris(1-phenyl-1-H-benzimidazole) (TPBi) and 2,9-dimethyl-4,7-diphenyl-1,10-phenanthroline (BCP) were used with the aim to decouple the efficacy of hole blocking from electron injection and transport. We obtained significantly improved optical performance with BCP which proved to be efficient hole blocking/electron injecting layer.

The 15 mm × 15 mm glass substrates were cleaned with Hellmanex soap in ultrapure water for 15 minutes in an ultrasonic bath, then were rinsed in pure water for 5 minutes two times. They were then subjected to 10 minutes of UV-O_3 treatment. Aluminum (100 nm) as gate was evaporated in an e-beam deposition system at the base pressure of 1×10^{-6} mbar. The aluminum was partially anodized in a citric acid aqueous solution (0.1 mM) to get 35 nm thick Al_2O_3. A thin polystyrene (3 mg mL^{-1} in chlorobenzene) layer was spin coated (2000 rpm, 60s) on top to passivate the surface. The transport

layer, C_{10}-DNTT (20nm), was evaporated in a thermal evaporator at the base pressure of 1×10^{-6} mbar with a controlled rate of 0.1 to 0.2 Å s^{-1}. MoO_3 (10nm)/Ag (40nm) source electrode was evaporated through a shadow mask at a deposition rate of 0.1 nm s^{-1}. The emissive layer, Alq_3 (50 nm), was evaporated thermally at a rate of 0.5 Å s^{-1}. Finally, the semitransparent drain electrode (LiF (1nm)/Al (15nm)) was evaporated through a shadow mask. Thus defined channel length was 300 µm and channel width was 2 mm. For BCP (10 nm) and TPBi (10 nm) devices, they were evaporated thermally at a rate of 0.1 nm s^{-1} before the deposition of drain electrode through the same shadow mask. The characterizations were carried out under inert atmosphere (nitrogen glovebox). A 4200 Keithley Semi-conductor analyzer along with a calibrated silicon photodetector on top of the device were used to measure the electrical and optical signals. A Hamamatsu amplifier was used to magnify the photocurrent. The brightness of Alq3 based OLED was first measured via a Konica Minolta Luminance meter LS-100. A correction factor was hence determined to derive the brightness of OLETs. Whole (LiF/Al) electrode area is considered as light emitting area to take into account the change in the area of the light emission. The photographs were taken by using a Nikon D-80 camera with a 50 mm lens.

First, we evaluated the OFET performance of C_{10}-DNTT molecule. Al gate deposited on glass substrate was partially anodized to create Al_2O_3, which served as dielectric layer. [27,28] A thin layer of polystyrene was spin coated to passivate the surface. [21] Subsequently, C_{10}-DNTT was deposited, followed by the deposition of MoO_3/Ag source/drain electrodes. [29] We obtained an average saturation hole mobility of 4.3 $cm^2 V^{-1} s^{-1}$, with low threshold voltage and high current on-off ratio (see supporting information). Such an excellent performance makes the choice of C_{10}-DNTT relevant as the transport layer of our OLETs. The OLET device structure is presented in Figure 1a). Here, we used asymmetric contacts for separate hole and electron injection. After the deposition of MoO_3/Ag contact for hole injection, Alq_3 emitter was thermally evaporated. The second asymmetric contact for electron injection is composed of hole blocking molecule (or not) and LiF/Al semi-transparent electrode. The choice of BCP and TPBi is mainly due to their deep lying highest occupied molecular orbital (HOMO) levels (6.2-6.4 eV), which enable them to block holes coming through the emissive layer in a rather similar fashion. For that, they both commonly act as hole blocking layers in OLEDs. [30] However, relatively large difference in lowest unoccupied molecular orbital (LUMO) levels (2.7 eV for TPBi and 3.0 eV for BCP) and in electron transport can manifest in their ability to efficiently provide electrons, thus influencing the rate of recombination that creates the excitons by the accumulation of both charges in the emissive layer. [31] We carried out experiments with different thicknesses and chose the best performing device (10 nm) in terms of current density and luminance for BCP device. We kept the thickness of TPBi the same for the sake of comparison, since TPBi devices get worse and worse than the reference device with the increase of the thickness.

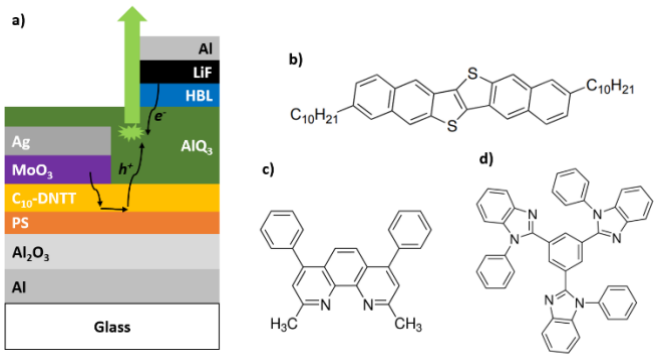

Fig. 1. a) Device structure of the OLET (PS: polystyrene, HBL: hole blocking layers TPBi or BCP). Chemical structures of b): C_{10}-DNTT, c): BCP and d): TPBi. MoO_3/Ag contact is grounded (source) and fixed V_{ds} is applied to the LiF/Al contact (drain) during the characterizations.

The electrical and optical characteristics of the three OLET devices (control, with TPBi and with BCP) are shown in Figure 2a) at a drain-source voltage (V_{ds}) of -5 V. All three devices show quite similar transfer curves, with comparable current turn on voltage (V_{on}(I)), threshold voltage (V_{th}) and maximum drain current (I_{max}). In contrast, we observed large differences in the optical performances. Maximum luminance of the device with BCP is almost ten times higher than that of the control device, indicating an efficient hole blocking by the BCP layer. However, despite having deeper HOMO level, TPBi device yielded even worse luminance than the control device. If we look at the energy diagram of various layers of our devices (as shown in Figure 2c)), shallow LUMO level of TPBi (2.7 eV) seems to introduce additional energetic barrier for electron injection from LiF/Al contact to Alq_3. Apparently, electron injection has stronger effect than hole blocking. Another factor to be considered is the electron mobility of these two HBLs. Earlier reports have shown that BCP has much higher electron mobility than TPBi. [32,33] Having almost one order of magnitude higher electron mobility, BCP transports electrons much faster than TPBi, which can be another contributing factor for the better performance of BCP device.

Device performances measured at drain-source voltage of -15 V are presented in Figure 2b). Remarkably, V_{on}(I) and light turn on voltage (V_{on}(L)) almost overlap for all the devices, which is a strong contrast to the solution processed hybrid LETs. [34,35] The hole transport layer (C_{10}-DNTT) is the same for all the control, TPBi and BCP devices. In principle they should have similar hole mobilities. Nevertheless, more efficient electron injection can lead to higher recombination rate in the emissive layer, thus further contributing to the current flow. Thus, we obtained a slightly higher mobility for BCP devices when operated at 15 V. Still, the mobility values are comparable to the OFET without the emissive layer. Maximum gate leakage current is around 2 nA, and several orders magnitude lower than the corresponding drain current (see supporting information). Overall optical performances follow the trend observed earlier for low voltage operation, albeit being less significant. Peculiar feature in the control device where a dip appears around gate voltage of 7.5 V is worthy of discussion.

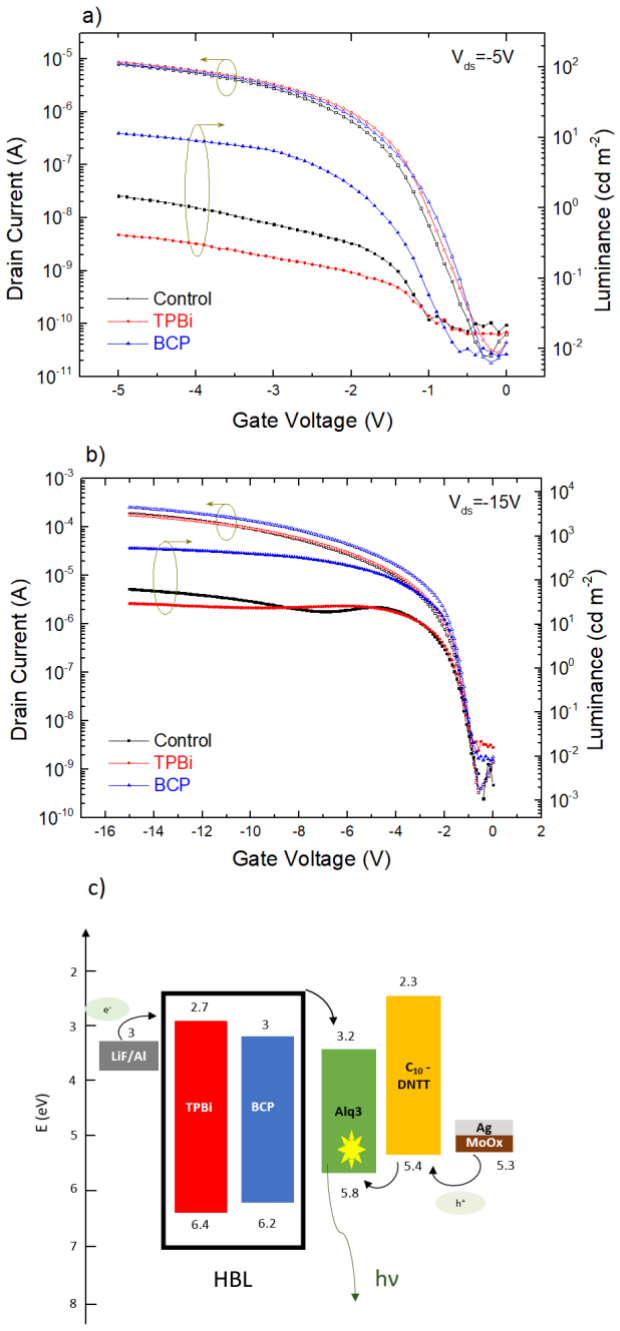

Fig. 2. a) Transfer characteristics and luminance of control, TPBi and BCP OLETs operating at V_{ds}=-5V. b) Transfer characteristics and luminance of control, TPBi and BCP OLETs operating at V_{ds}=-15V. c) Energy diagram of various layers with respect to the vacuum level.

We should note that when the gate voltage increases, the carrier concentration of the holes continues to rise, conversely that of the electrons continues to diminish, as it is controlled by the potential difference between the gate electrode and drain electrode (LiF/Al). The equilibrium point is at half gate voltage, where the switch from electron domination to hole domination occurs. At high gate voltages, electron injection is predominantly through tunnelling, driven by the fixed electric field between source and drain electrode over the channel. When electron injection/transport is poor, as

in the case of TPBi devices, the increased amount of hole carriers through efficient blockage are compensated, hindering further accumulation of electron/hole pairs (excitons) in the emissive layer. When electron injection gets better, as in the case of control device, exciton accumulation improves, leading to still enhanced luminance after the switching point for hole domination. The best case is BCP, where continuous enhancement of exciton accumulation is achieved thanks to both efficiently blocked holes and injected/transported electrons. Such luminance characteristics at high gate voltage region again confirm the importance of electron injection/transport abilities of these HBLs. Brightness higher than 700 cd m^{-2} is obtained for BCP device operating at -15 V. Output characteristics of the devices are provided in the supporting information. Current efficiencies of the devices are also given in the supporting information. Electrical and optical performance parameters are summarized in Table I.

Table I. Summary and comparison of electrical and optical properties of control, TPBi and BCP OLETs at V_{ds} of -5 V. The values in the brackets are for the operation at V_{ds} of -15 V.

	control	TPBi	BCP
Max. mobility ($cm^2 V^{-1} s^{-1}$)	2.5 ± 0.8 (3.3 ± 0.9)	2.2 ± 0.7 (3.4 ± 1)	2.2 ± 0.3 (4 ± 0.5)
Current on/off ratio	4×10^5 (5×10^5)	4×10^5 (5×10^5)	4×10^5 (2×10^6)
Threshold voltage-V_{th} (V)	-1.2 ± 0.1 (-1.2 ± 0.1)	-0.9 ± 0.07 (-1 ± 0.1)	-1 ± 0.1 (-1.2 ± 0.2)
Current turn on voltage-V_{on}(I) (V)	-0.5 ± 0.1 (-0.6 ± 0.05)	-0.3 ± 0.1 (-0.5 ± 0.1)	-0.4 ± 0.1 (-0.6 ± 0.1)
Light turn on voltage-V_{on}(L) (V)	-0.8 ± 0.1 (-0.7 ± 0.06)	-0.5 ± 0.2 (-0.6 ± 0.1)	-0.7 ± 0.1 (-0.7 ± 0.1)
Max. brightness (cd m^{-2})	1.6 ± 1 (50 ± 10)	0.4 ± 0.09 (30 ± 7)	10 ± 4 (633 ± 113)

Visual observation of the emitted lights from the three devices operating at -15 V are presented in Figure 3 for the control device, the device with TPBi and the device with BCP (a), b) and c)). These photograph images show that the lights are emitted primarily from LiF/Al electrode edge, which is due the high concentration of the excitons near the channel. We actually noticed that light emission started from the edge, slowly diffusing the area under the electrode with the increase of the gate voltage, revealing exciton distribution profile. It is also evident that BCP device is brighter than control and TPBi devices, in agreement with the luminance measurement data. However, a closer look exposes the differences in the colour of the emitted lights of the three devices. To verify that, we recorded electro-luminance (EL) spectra and compared them with photo-luminance (PL) spectrum of Alq_3 film, as shown in Figure 3d). The main EL peak at 520 nm of all the three devices corresponds to that of the PL peak of Alq_3 film. Interestingly, we observed additional red shifted EL peaks. The position of this optical resonance seems to be related to the distance between Al gate electrode and Al top electrode. With 10 nm more thickness due to the HTLs, the peak shifted from 610 nm in the control device to

660 nm for the devices with BCP and TPBi. Such a phenomenon was not observed in Si/SiO_2 high operating voltage based devices. The origin of this optical effect is the subject of our further study.

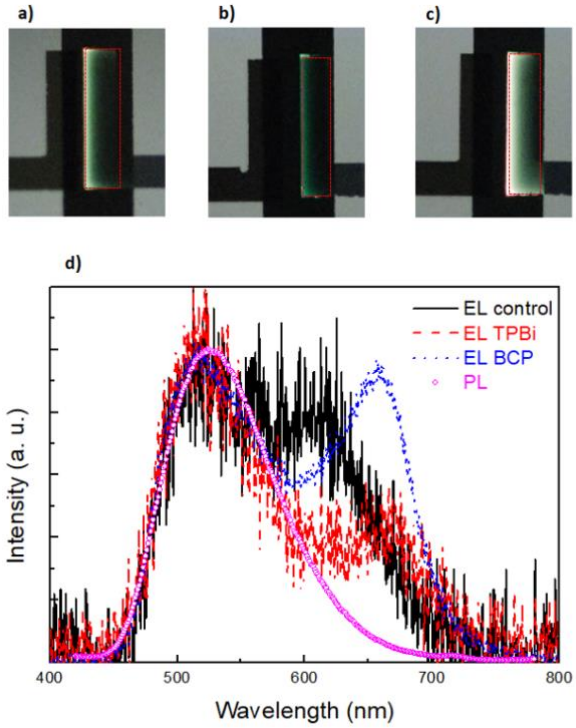

Fig. 3. Photographs of the light emission from OLET devices (LiF/Al electrodes are designated with dashed red lines): a) control, b) with TPBi and c) with BCP. d) Electroluminescence (EL) spectra of the same OLET devices together with photoluminescence (PL) spectrum of Alq_3 film.

In summary, we presented Alq_3 emissive layer based OLETs operating at as low as 5 V, which were realised by adopting C_{10}-DNTT high mobility transport layer and anodized Al_2O_3 high capacitance dielectric layer. These devices allowed us to investigate the role of hole blocking molecules in these OLETs. Two molecules, BCP and TPBi, were compared, in order to distinguish the separate mechanisms of hole blocking and electron injection/transport. Baring more suitable energy level for electron injection and higher electron mobility, BCP resulted in much improved optical performance than the control and TPBi devices. On the contrary, TPBi displayed even worse performance than control device. Thus, we identified that in low voltage operating OLETs, merely efficient hole blocking is not sufficient to enhance device performance without decent electron injection/transport. Low operating voltage OLETs with efficient charge blocking layer usher these important optoelectronic devices closer to many potential practical applications, on which our study provides one of the roadmaps.

Acknowledgment. A. Bachelet acknowledges financial support of Université Bordeaux Doctoral Grant and A. Ablat from the French national PAUSE program.

References

1. Forrest, S. R. The path to ubiquitous and low-cost organic electronic appliances on plastic. *Nature* **428**, 911–918 (2004).
2. Khan, Y. *et al.* A New Frontier of Printed Electronics: Flexible Hybrid Electronics. *Adv. Mater.* 1905279 (2019) doi:10.1002/adma.201905279.
3. Wang, G., Adil, M. A., Zhang, J. & Wei, Z. Large-Area Organic Solar Cells: Material Requirements, Modular Designs, and Printing Methods. *Adv. Mater.* **31**, 1805089 (2019).
4. Kaltenbrunner, M. *et al.* Ultrathin and lightweight organic solar cells with high flexibility. *Nat. Commun.* **3**, 770 (2012).
5. Yin, D. *et al.* Highly Flexible Fabric-Based Organic Light-Emitting Devices for Conformal Wearable Displays. *Adv. Mater. Technol.* 1900942 (2020) doi:10.1002/admt.201900942.
6. Muccini, M. A bright future for organic fi eld-effect transistors. *Nat. Mater.* **5**, 605–613 (2006).
7. Chaudhry, M. U. *et al.* Organic Light-Emitting Transistors: Advances and Perspectives. *Adv. Funct. Mater.* 1905282 (2019) doi:10.1002/adfm.201905282.
8. McCarthy, M. A. *et al.* Low-voltage, low-power, organic light-emitting transistors for active matrix displays. *Science (80-.).* **332**, 570–573 (2011).
9. Kuehne, A. J. C. & Gather, M. C. Organic Lasers : Recent Developments on Materials , Device Geometries , and Fabrication Techniques. *Chem. Rev.* **116**, 12823−12864 (2016).
10. Hepp, A. *et al.* Light-emitting field-effect transistor based on a tetracene thin film. *Phys. Rev. Lett.* **91**, 157406 (2003).
11. Gwinner, M. C. *et al.* Highly efficient single-layer polymer ambipolar light-emitting field-effect transistors. *Adv. Mater.* **24**, 2728–2734 (2012).
12. Sobus, J. *et al.* High Performance p- and n-Type Light-Emitting Field-Effect Transistors Employing Thermally Activated Delayed Fluorescence. *Adv. Funct. Mater.* **28**, 1800340 (2018).
13. Liu, C. F., Liu, X., Lai, W. Y. & Huang, W. Organic Light-Emitting Field-Effect Transistors: Device Geometries and Fabrication Techniques. *Adv. Mater.* **30**, 1–34 (2018).
14. Yuan, D., Sharapov, V., Liu, X. & Yu, L. Design of High-Performance Organic Light-Emitting Transistors. *ACS Omega* **5**, 68–74 (2020).
15. Ullah, M., Wawrzinek, R., Nagiri, R. C. R., Lo, S. & Namdas, E. B. UV–Deep Blue–Visible Light-Emitting Organic Field Effect Transistors with High Charge Carrier Mobilities. *Adv. Opt. Mater.* **5**, 1600973 (2017).
16. Hsu, B. B. Y. *et al.* Ordered polymer nanofibers enhance output brightness in bilayer light-emitting field-effect transistors. *ACS Nano* **7**, 2344–2351 (2013).
17. Maruyama, K. *et al.* Ambipolar light-emitting organic single-crystal transistors with a grating resonator. *Sci. Rep.* **5**, 10221 (2015).
18. Kyndiah, A. *et al.* A Multifunctional Interlayer for Solution Processed High Performance Indium Oxide Transistors. *Sci. Rep.* **8**, 10946 (2018).
19. Zschieschang, U. *et al.* Dinaphtho[2,3-b:2',3'-f]thieno[3,2-b]thiophene (DNTT) thin-film transistors with improved performance and stability. *Org. Electron. physics, Mater. Appl.* **12**, 1370–1375 (2011).

20. Chen, H. *et al.* Dithiopheneindenofluorene (TIF) Semiconducting Polymers with Very High Mobility in Field-Effect Transistors. *Adv. Mater.* **29**, 1702523 (2017).
21. Houin, G. *et al.* Device Engineering for High Performance, Low Voltage Operating Organic Field Effect Transistor on Plastic Substrate. *Flex. Print. Electron.* **2**, 45004 (2017).
22. Ortiz, P., Facchetti, A. & Marks, T. J. High- k Organic , Inorganic , and Hybrid Dielectrics for Low-Voltage Organic Field-Effect Transistors. *Chem. Rev.* **110**, 205–239 (2010).
23. Chaudhry, M. U. *et al.* Low-Voltage Solution-Processed Hybrid Light-Emitting Transistors. *ACS Appl. Mater. Interfaces* **10**, 18445–18449 (2018).
24. Fahlman, M. *et al.* Interfaces in organic electronics. *Nat. Rev. Mater.* **4**, 627–650 (2019).
25. Soldano, C., D'Alpaos, R. & Generali, G. Highly Efficient Red Organic Light-Emitting Transistors (OLETs) on High-k Dielectric. *ACS Photonics* **4**, 800–805 (2017).
26. Kang, M. J. *et al.* Alkylated dinaphtho[2,3-b:2',3'-f]thieno[3,2-b]thiophenes (Cn-DNTTs): Organic semiconductors for high-performance thin-film transistors. *Adv. Mater.* **23**, 1222–1225 (2011).
27. Abbas, M. *et al.* Water soluble poly(1-vinyl-1,2,4-triazole) as novel dielectric layer for organic field effect transistors. *Organic Electronics* vol. 12 497–503 (2011).
28. Dang, X. D., Plieth, W., Richter, S., Plötner, M. & Fischer, W. J. Aluminum oxide film as gate dielectric for organic FETs: Anodization and characterization. *Phys. Status Solidi Appl. Mater. Sci.* **205**, 626–632 (2008).
29. Ablat, A. *et al.* Role of Oxide / Metal Bilayer Electrodes in Solution Processed Organic Field Effect Transistors. *Sci. Rep.* **9**, 6685 (2019).
30. Jou, J. H. *et al.* Carrier modulation layer-enhanced organic light-emitting diodes. *Molecules* **20**, 13005–13030 (2015).
31. Jou, J. H. *et al.* Highly efficient color-temperature tunable organic light-emitting diodes. *J. Mater. Chem.* **22**, 8117–8120 (2012).
32. Kulkarni, A. P., Tonzola, C. J., Babel, A. & Jenekhe, S. A. Electron Transport Materials for Organic Light-Emitting Diodes Abhishek. *Chem. Mater.* **16**, 4556–4573 (2004).
33. Rhee, S. H. *et al.* Effect of electron mobility of the electron transport layer on fluorescent organic light-emitting diodes. *ECS Solid State Lett.* **3**, 19–22 (2014).
34. Ullah, M. *et al.* Hybrid Light-Emitting Transistors Based on Low-Temperature Solution-Processed Metal Oxides and a Charge-Injecting Interlayer. *Adv. Opt. Mater.* **4**, 231–237 (2016).
35. Ablat, A. *et al.* Low optical turn-on voltage in solution processed hybrid light emitting transistor. *Appl. Phys. Lett.* **115**, 023301 (2019).